

Simultaneous Ionization and Excitation of Neon by Electron Impact*

Keith G. Walker[†] and Robert M. St. John

Department of Physics and Astronomy, University of Oklahoma, Norman, Oklahoma 73069

(Received 2 February 1972)

The simultaneous ionization and excitation cross sections by electron impact for the $3p$, $3d$, and $4s$ levels in neon of the 3P , 1D , and 1S cores have been examined. The excitation functions were quite broad. In all, over 100 optical cross sections have been measured and over 50 excitation functions from threshold to 1000 eV were obtained. The cascade lines from the $3d$ and $4s$ levels of the various cores were very weak, with some at the limit of detectability. The error of these cascade cross sections ranges from 10 to 50%. The direct-excitation cross sections were obtained for the $3p$ levels of the three cores. Polarization effects were examined and only three levels exhibited any polarization; these were less than 10%. There are no previous experimental measurements of these cross sections. The branching ratios obtained by experiment and calculation have been compared with those yielded by our work. These branching ratios, the lack of strong lines between doublet and quartet levels, and the general tendency of the quartet excitation functions to be more peaked than the doublets leads us to accept the $(^3P)3p$ levels as being well designated by LS coupling. In conjunction with this and the exceptionally broad excitation functions, it appears that the ionization cross section influences the energy dependence of the simultaneous ionization and excitation cross section. The high-energy portion of the excitation functions tended to bear this out as well. The sudden-perturbation approximation has been applied to several of the $3p$ levels; its numerical values for the cross sections were two or three times greater than the experimental values. The cross section of most observed levels falls off with electron energy E as E^{-1} . Theory tends to indicate a $(\ln E)/E$ dependence at high energy.

INTRODUCTION

The frequency with which neon is utilized in high-temperature gaseous devices, astrophysical observations, and of late, lasers has prompted the need for collision information. Not until recently has such information been available. Sharpton *et al.*¹ have studied to great extent the electron impact excitation of atomic neon both experimentally and theoretically. We have conducted an investigation of electron excitation of the neon atoms to their ion states by a single electron impact. Several of these ion levels have been found as upper laser levels² and are of particular interest.

This paper contains the absolute cross sections for simultaneous ionization and excitation to the $3p$ levels of Ne II with cascade contributions from the $3d$ and $4s$ levels. Optical excitation functions have been obtained from threshold to 1000 eV. The data are compared with available theoretical calculations.

One of the difficulties encountered in this study was the obtainment of an accurate classification of spectral transitions for the singly ionized states of neon. Some of the assignments of $3d$ and $4f$ levels of early publications were doubtful. Published results for the line strengths for Ne II transitions utilized these early assignments and hence are subject to error. Persson and Minnhagen³ have made a partial analysis of the spectrum of Ne II

and have corrected many of the assignments and classified newly found transitions. A complete analysis of the spectrum of Ne II by Persson⁴ has just been published since we made our assignments. Through private communication with Persson our line assignments are in agreement with his latest results.

EXPERIMENTAL METHOD

The experiment consists of subjecting a gas of known density to an electron beam which is well defined, both geometrically and energetically. The resulting collisions produce atoms in an excited state. The rate of depopulation by spontaneous emission is betrayed by the radiation from the excited level j to all allowed lower levels. If the total photon flux from the interaction region due to transitions from level j is measured, then we possess a quantity which expresses the number of atoms which must be entering level j each second. This assumes that no nonradiating channels of decay exist such as multiple electron collisions or atom-atom collisions with a subsequent energy exchange. To ensure the validity of such assumptions, a linear relationship was established between the monitored photon flux and the gas and electron densities.

The photon flux F_{jk} due to the $j \rightarrow k$ transition is

$$F_{jk} = Q_{jk}(I/e)NL, \quad (1)$$

where I is the electron beam current, e the elec-

tronic charge, N is the gas density, L is the length of the collision area from which radiation is gathered, and Q_{jk} is designated as the *optical cross section* of the $j \rightarrow k$ transition. F_{jk} is obtained absolutely by standardizing the detection system with a tungsten-ribbon standard lamp. The details of this standardization process are given in previous papers^{1,5} and will not be repeated here.

The sum of all the photon fluxes from level j gives rise to the *apparent cross section* Q'_j which is defined by

$$F_j \equiv \sum_k F_{jk} = (I/e)NL \sum_k Q_{jk}, \quad (2)$$

$$Q'_j \equiv \sum_k Q_{jk} = \frac{F_j}{(I/e)NL}. \quad (3)$$

Since part of the population of level j is due to cascade from higher levels, we must subtract the photon flux of those transitions terminating on level j in order to determine the cross section for direct electron excitation. We have

$$\frac{F_j}{(I/e)NL} - \frac{\sum_i F_{ij}}{(I/e)NL} = Q'_j - \sum_i Q_{ij} \quad (4)$$

and

$$Q_j = \sum_k Q_{jk} - \sum_i Q_{ij}, \quad (5)$$

where Q_j is termed the *level cross section* of the j th state.

The electron gun is similar to that described by Jobe and St. John.⁶ The electron beam is 3 mm in diam with an electron current capability of 10^{-3} A. However, the current used in this experiment was 500 μ A. The energy resolution of this gun was found to be 0.4 to 0.5 eV from excitation thresholds and resonant features in helium and neon. The apparatus for detecting the radiation and measuring relative excitation functions is similar to

that displayed in Fig. 1 of Ref. 1. The radiation was viewed at right angles to the electron beam. The detecting portion of the apparatus is a Jarrell-Ash $\frac{1}{2}$ -m monochromator coupled to an EMI 6256B photomultiplier tube. The radiation was chopped mechanically before it entered the monochromator. This coupling was accomplished by a bladed synchronous motor which was driven by the reference output signal of a lock-in amplifier. The photomultiplier tube signal was amplified by the same lock-in amplifier. The dc output of the lock-in amplifier was fed to the vertical deflecting plates of an oscilloscope. The horizontal sweep was driven by the accelerating voltage of the electron beam whose current was kept constant. The resulting curve displays Q' as a function of electron energy and is termed an *optical excitation function*. Absolute optical cross sections were measured at a predetermined fixed electron energy. The intensity of a line was recorded on a time-base chart recorder. This intensity was then compared with the intensity from a tungsten-ribbon-filament lamp whose photon flux for various filament temperatures has been standardized by the manufacturer with measurements traceable to the National Bureau of Standards. From these data, the absolute optical cross section of a transition can be obtained at that particular electron energy. These data in conjunction with the optical excitation functions give the absolute optical cross section at any energy covered by the excitation function.

Since the radiation was viewed perpendicularly to the electron beam, polarization of the emitted radiation must be considered. The perpendicular and parallel components of the radiation with respect to the electron beam were examined as well as the polarization effects of the monochromator. With the exception of three transitions (3727.1,

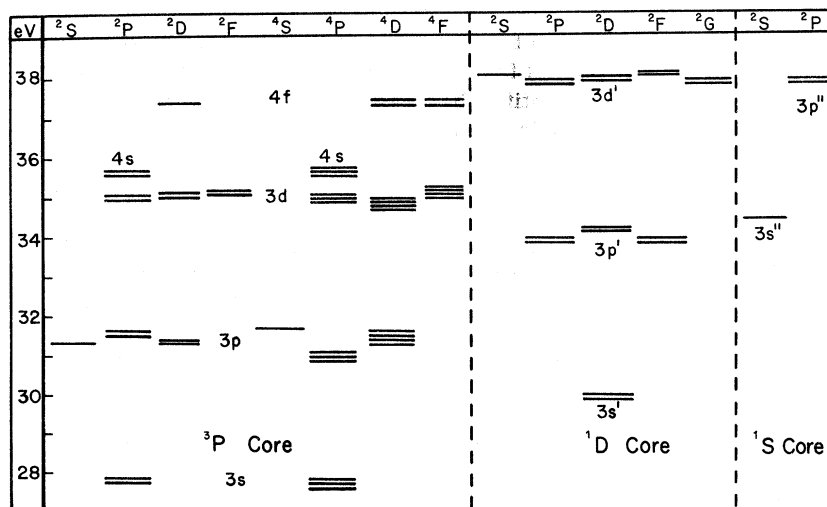


FIG. 1. Energy level diagram for singly ionized neon (Ne II).

3713.1, and 3334.8 Å), the magnitude of the polarization was less than 5%. The three exceptions had a maximum polarization between -5 and -10% in the vicinity of 90 eV. As a check on our method and procedure for polarization measurements, the polarization of the 4^1D-2^1P line of helium was examined and compared with measurements taken by Clout and Heddle.⁷ Our results were identical to theirs out to 100 eV. From 100 to 300 eV, our results were about 3-5% higher.

Ultrahigh-vacuum techniques were employed throughout. Spectroscopically pure neon was passed over liquid nitrogen before its introduction to the collision chamber. Also, a nonevaporable getter pump was utilized to pump impurities boiled off the cathode and any other contaminants in the system. Since this pump offers the feature that it possesses absolutely no affinity for the inert gases, but will readily pump the active gases, a static system was possible enabling an accuracy of $\frac{1}{2}\%$ in the pressure measurement by a capacitance monometer. The pressure range for this investigation, 10 to 20 mTorr, yielded a linear relation-

ship between signal and electron current.

RESULTS

Figure 1 is the energy-level diagram for Ne II. The energy scale is referred to the ground state of the ion. The ground state of the ion is a $2s^2 2p^5$ configuration which gives rise to a 2P term. The excited Ne II configuration can be expressed as $2s^2 2p^4 nl$, where $2s^2 2p^4$ represents the core and nl the configuration of the running electron. The $2s^2 2p^4$ core configuration, based on the LS coupling scheme, contains three different terms: 3P , 1D , and 1S . The 3P core coupled to the excited electron generates a doublet and quartet system. The 1D and 1S cores, when associated with the excited electron, each give only a doublet system. We present herein the optical, apparent, and level excitation cross sections for simultaneous ionization and excitation of the $3p$ levels (associated with 3P core), the $3p'$ levels (associated with 1D core), and $3p''$ levels (associated with 1S core). The cascade into these levels has been measured from the $3d$ and $4s$ levels of each core and is es-

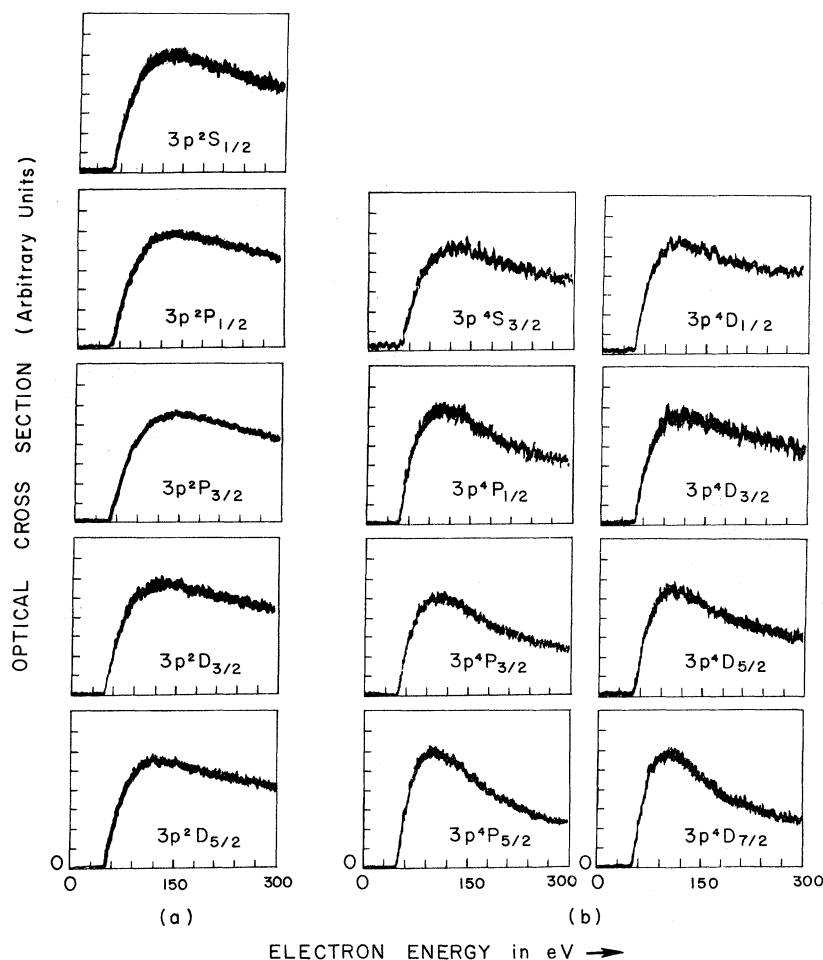


FIG. 2. Optical excitation functions of the $3p$ levels. (a) Doublets, (b) quartets.

TABLE I. Optical cross sections Q_{jk} of the spectral lines for the $3s-3p$ series at 150 eV in units of 10^{-21} cm².

Transition	Line (Å)	Q_{jk}
$^2P_{1/2}-^2S_{1/2}$	3557.81	1.6
$^2P_{3/2}-^2S_{1/2}$	3481.94	8.3
$^2P_{1/2}-^2P_{1/2}$	3378.21 ^a	71.1
$^2P_{3/2}-^2P_{1/2}$	3309.74	11.0
$^2P_{1/2}-^2P_{3/2}$	3392.79 ^a	39.7
$^2P_{3/2}-^2P_{3/2}$	3323.74 ^a	130.0
$^2P_{1/2}-^2D_{3/2}$	3727.10	18.4
$^2P_{3/2}-^2D_{3/2}$	3643.93	5.5
$^2P_{3/2}-^2D_{5/2}$	3713.08	27.0
$^4P_{1/2}-^4S_{3/2}$	3028.86	1.3 ^b
$^4P_{3/2}-^4S_{3/2}$	3001.67	2.2
$^4P_{5/2}-^4S_{3/2}$	2955.72	2.8
$^4P_{1/2}-^4P_{1/2}$	3751.25	1.3
$^4P_{3/2}-^4P_{1/2}$	3709.62	7.0
$^4P_{1/2}-^4P_{3/2}$	3777.13	5.7
$^4P_{3/2}-^4P_{3/2}$	3734.94	2.4
$^4P_{5/2}-^4P_{3/2}$	3664.07	8.2
$^4P_{3/2}-^4P_{5/2}$	3766.26	4.9
$^4P_{5/2}-^4P_{5/2}$	3694.21	15.4
$^4P_{1/2}-^4D_{1/2}$	3344.40	6.1
$^4P_{3/2}-^4D_{1/2}$	3311.27	1.0
$^4P_{1/2}-^4D_{3/2}$	3360.60	5.2
$^4P_{3/2}-^4D_{3/2}$	3327.15 ^a	6.6
$^4P_{5/2}-^4D_{3/2}$	3270.80	0.4
$^4P_{3/2}-^4D_{5/2}$	3355.01	12.9
$^4P_{5/2}-^4D_{5/2}$	3297.73	3.5
$^4P_{5/2}-^4D_{7/2}$	3334.83	15.7

^aObserved laser line (Ref. 2).

^bThis cross section was determined by use of experimental branching-ratio data of Hodges (Ref. 14) as the line could not be resolved.

estimated to amount to 90% of the total cascade.

A. 3P Core

Figure 2 displays the optical excitation functions from threshold to 300 eV for the $3p$ levels of the 3P core. Table I contains the absolute optical cross sections for transitions originating from these levels. Each result represents the average of six measurements. The repeatability of a single measurement depends on the intensity of the line and the corresponding signal-to-noise ratio of the instruments. The strong lines have a repeatability to within 1 or 2%, while some of the very weak cascade lines to be presented later had a repeatability variation of 20 to 30%. An error analysis of the various measuring devices yields an experimental error which can be applied to the average of the cross-section measurements. In this analysis we considered the errors associated with the measurement of the pressure ($\frac{1}{2}\%$), with the electron current ($\frac{1}{2}\%$), with the electron en-

ergy ($\frac{1}{2}\%$), with the gain factors for the various amplifiers and zero drift (3%), with the dimensions of various apertures and other geometric factors necessary for standardization (1%), and standard lamp current ($\frac{1}{2}\%$). This amounts to 6% and does not include the uncertainties in the emissivity values of tungsten measured by DeVos⁸ and the calibration of the temperature of the standard lamp with current. An estimate of 10% for these two sources of error is liberal. Hence, a total experimental error of the average cross-section values of 15% is viewed as reasonable.

The transition $3p\ ^4S_{3/2}-3s\ ^4P_{1/2}$ at 3029 Å was not resolvable from a weak neighboring line; hence, a branching ratio was used to determine its intensity. Several sources of branching ratios are available. Garstang⁹ has calculated the line strength for numerous Ne II transitions, obtaining values for LS and intermediate-coupling schemes. The transition probabilities can then be calculated from these line strengths by the standard formulas.¹⁰ Koozekanani and Trusty¹¹ and Luyken¹² have made similar calculations. Koopman¹³ and Hodges *et al.*¹⁴ have measured the line strengths experimentally.

For selecting the branching ratios which were used, the following procedure was adopted. All branching ratios obtainable from the data of this work were compared to those of the other sources. That source which agreed best with our results was used. We obtained 40 branching ratios which we compared with the experimental results of Koopman and of Hodges; those of Hodges compared most favorably to ours. Therefore, the cross section for the 3029-Å line was obtained using Hodges's data. The value of 1.3×10^{-21} cm² so calculated compares well with our experimental values of 1.4×10^{-21} cm² for this line and the weak unresolved adjacent line.

The cascade into the $3p$ levels originates for the most part from the $3d$ and $4s$ levels. Figure 3 shows the optical excitation functions for these $3d$ and $4s$ levels. Some of the quartet cascade lines were so weak that it was not possible to obtain their excitation functions. In general, the excitation functions of the cascade levels have a shape similar to the $3p$ levels. This results in very little change in the shape of the $3p$ excitation functions when cascade is subtracted.

The optical cross sections for these cascade transitions are presented in Table II. Several lines were unresolvable and/or so weak that they were beyond the detectability of the present system (10^{-22} cm²). Therefore, branching ratios were used in obtaining some of the results. The branching ratios obtained from the work of Hodges *et al.* were used where possible. Otherwise, Garstang's intermediate-coupling calculations were used.

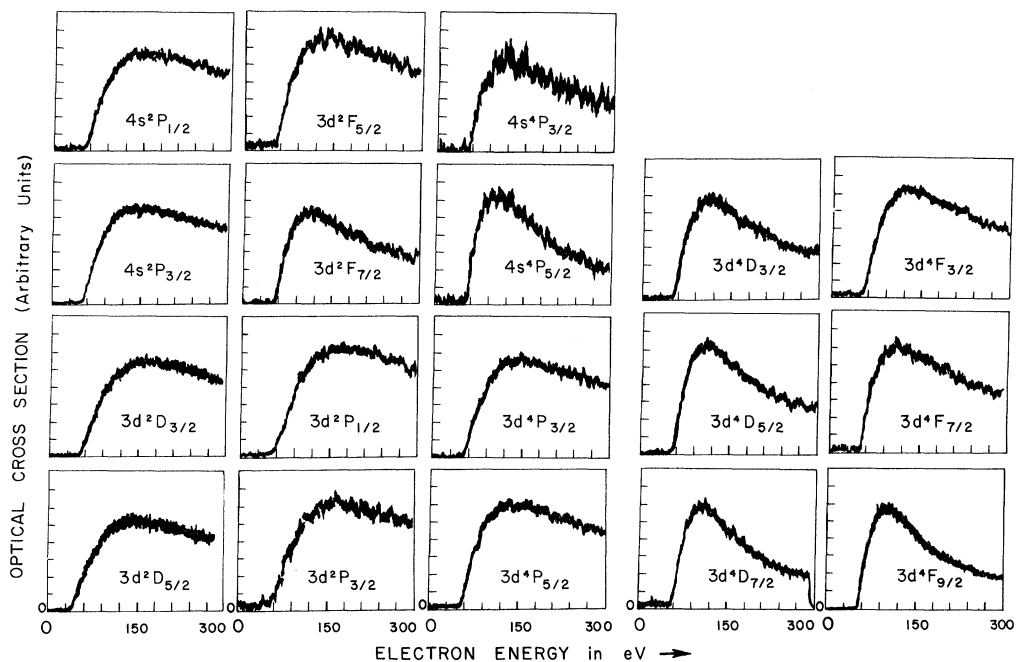
FIG. 3. Optical excitation functions of the $3d$ and $4s$ levels.B. 1D Core

Figure 4 shows the optical excitation functions for the six $3p'$ levels of this core. The $3p' 2P_J$

levels are particularly broad and appear almost flat for energies beyond the maximum. Also the rise after onset is very slow with energy.

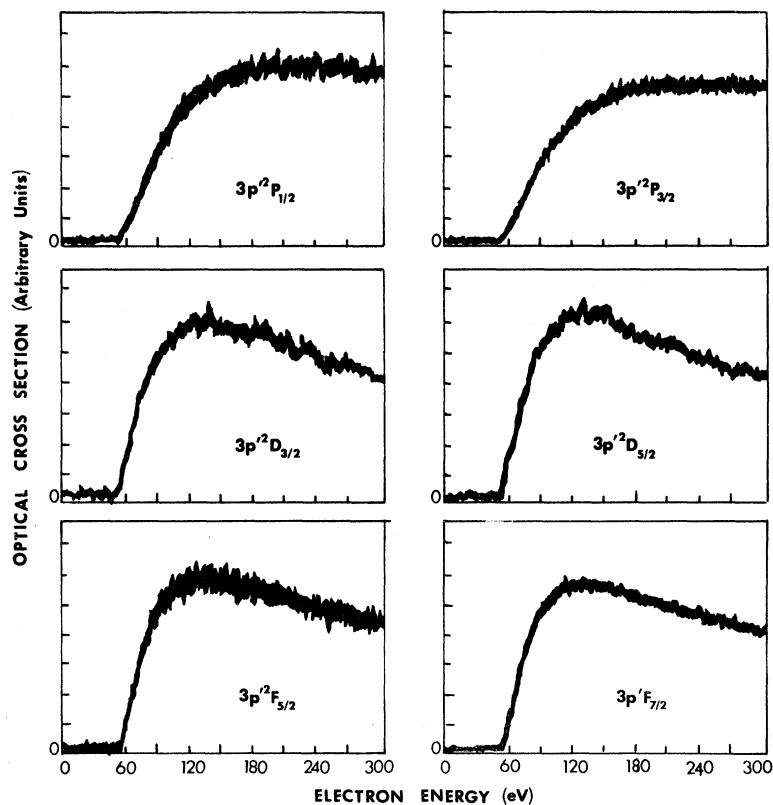
FIG. 4. Optical excitation functions of the $3p'$ level.

TABLE II. Optical cross sections Q_{jk} of the spectral lines for the $3p$ - $3d$ and $3p$ - $4s$ series at 150 eV in units of 10^{-21} cm². Cross sections in parentheses were obtained using branching ratios from Garstang's intermediate-coupling calculations (Ref. 9). Cross sections in brackets were obtained using branching-ratio data of Hodges (Ref. 14).

Lower level	Upper level							Upper level							Upper level								
	3d							4s							3d			4s					
	² P _{1/2}	² P _{3/2}	² D _{3/2}	² D _{5/2}	² F _{5/2}	² F _{7/2}		² P _{1/2}	² P _{3/2}	⁴ P _{1/2}	⁴ P _{3/2}	⁴ P _{5/2}	⁴ D _{3/2}	⁴ D _{5/2}	⁴ D _{7/2}	⁴ F _{3/2}	⁴ F _{5/2}	⁴ F _{7/2}	⁴ F _{9/2}	⁴ P _{1/2}	⁴ P _{3/2}	⁴ P _{5/2}	
² S _{1/2}	0.9	(1.5)	0.4						0.7														
² P _{1/2}	0.2	1.3	0.9					0.3	1.9		0.3												
² P _{3/2}	0.3	0.6	0.6	1.8	0.3				2.2														
² D _{3/2}			0.4	0.7	2.3				0.5		1.0							0.4					
² D _{5/2}		(0.2)		0.8	(0.6)	2.5			3.9														
⁴ S _{3/2}			0.2	1.0					0.6	0.9	2.7							1.3					
⁴ P _{1/2}									0.2	(0.8)				[0.8]						[0.2]	[0.6]		
⁴ P _{3/2}									(0.7)	(0.1)	[1.0]	1.5	1.9							[0.7]	[0.3]	0.5	
⁴ P _{5/2}									(0.5)	[1.0]	[0.6]	1.4	[4.5]								0.4	[1.3]	
⁴ D _{1/2}			0.4						(0.6)														
⁴ D _{3/2}				0.7	0.4				1.0	[0.2]	0.3				[0.7]	3.5				[1.1]	[0.5]	[0.4]	
⁴ D _{5/2}									(0.2)	(0.5)	(0.2)	0.7			0.6	2.7				1.2	[0.3]		
⁴ D _{7/2}										(0.9)		(0.1)	1.7		(0.3)	4.4						1.2	
Q'	1.4	3.6	2.7	4.2	4.6	2.5	0.3	9.2	1.5	4.4	7.3	3.4	4.1	6.2	4.0	4.5	3.0	4.4	2.8	3.0	3.7		

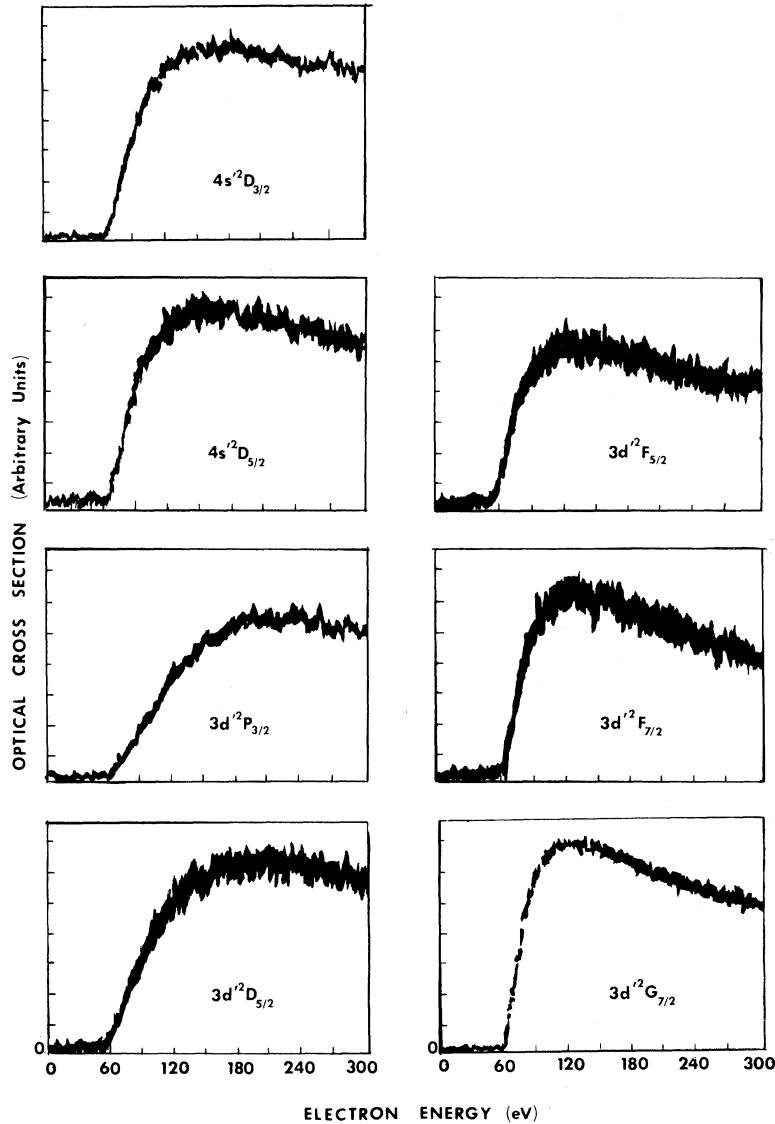


FIG. 5. Optical excitation functions of the $4s'$ and $3d'$ levels.

TABLE III. Optical cross sections Q_{jk} of the spectral lines for the $3s'-3p'$ series at 150 eV in units of 10^{-21}cm^2 .

Transition	Line (Å)	Q_{jk}
$^2D_{3/2}-^2P_{1/2}$	3319.72 ^a	47.6
$^2D_{3/2}-^2P_{3/2}$	3345.83	16.8
$^2D_{5/2}-^2P_{3/2}$	3345.45 ^a	76.4
$^2D_{3/2}-^2D_{3/2}$	3232.37	14.9
$^2D_{5/2}-^2D_{3/2}$	3232.02	1.7 ^b
$^2D_{3/2}-^2D_{5/2}$	3230.42	17.0
$^2D_{5/2}-^2D_{5/2}$	3230.07	1.6
$^2D_{3/2}-^2F_{5/2}$	3574.62	26.0
$^2D_{5/2}-^2F_{5/2}$	3574.18	1.9 ^b
$^2D_{5/2}-^2F_{7/2}$	3568.50	35.7

^aObserved laser line (Ref. 2).

^bCross section was determined by use of experimental branching-ratio data of Koopman (Ref. 13) as the line was too weak for direct determination.

The optical cross sections for those lines originating from the $3p'$ levels are given in Table III. The levels of a given doublet are quite close in this core and were barely resolvable. Since the slits of the monochromator were nearly closed, the weaker lines of the doublets were not detectable and only the stronger lines were measured. The weaker lines were obtained with branching ratios in the manner used for the 3P core. The $3p' \ ^2P_{1/2}$ and $3p' \ ^2P_{3/2}$ are upper laser levels in a neon-ion laser.

The number of cascade levels in this core configuration is much smaller than in the 3P core. The excitation functions of the $4s'$ and $3d'$ levels which could be obtained are presented in Fig. 5.

Table IV gives the optical cross sections at 150 eV for those cascade lines which could be measured.

C. 1S Core

Since only a single $3s''$ level exists, the apparent and optical cross sections are identical and have the values at 150 eV of $7.4 \times 10^{-21} \text{cm}^2$ and

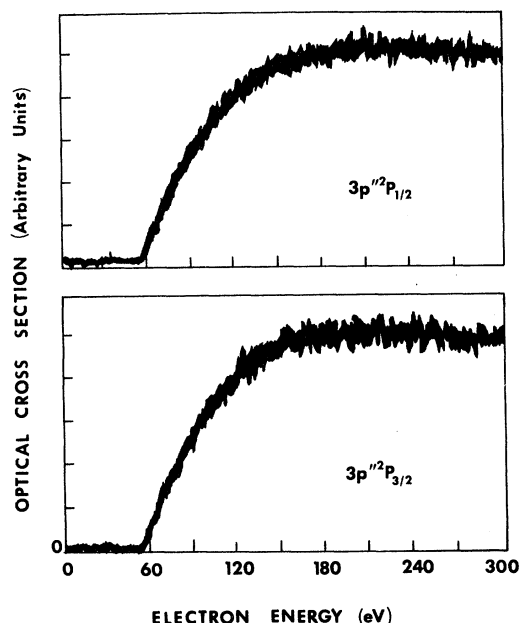


FIG. 6. Optical excitation functions of the $3p''$ levels.

$13.7 \times 10^{-21} \text{cm}^2$ for $3p'' \ ^2P_{1/2}$ and $3'' \ ^2P_{3/2}$, respectively. The optical excitation functions are presented in Fig. 6.

These functions are exceptionally broad, having features similar to those of $3p' \ ^2P_{1/2}$ and $3p' \ ^2P_{3/2}$ functions. No cascade lines were detectable for this core.

D. Level Cross Sections

Table V gives the level cross sections of the $3p$, $3p'$, and $3p''$ levels. Also included in Table V is the percentage of the apparent cross section for that level which was contributed by cascade. A review of Tables II and IV will show that the cascade contribution to the quartet levels is the most heavily influenced by theoretical branching ratios.

TABLE IV. Optical cross sections Q_{jk} of the spectral lines for the $3p'-3d'$ and $3p'-4s'$ series at 150 eV in units of 10^{-21}cm^2 .

Upper level		$3d'$							$4s'$		
Lower level		$^2S_{1/2}$	$^2P_{1/2}$	$^2P_{3/2}$	$^2D_{3/2}$	$^2D_{5/2}$	$^2F_{5/2}$	$^2F_{7/2}$	$^2G_{7/2}$	$^2D_{3/2}$	$^2D_{5/2}$
$3p'$	$^2P_{1/2}$	0.3	0.2	0.2 ^a							
	$^2P_{3/2}$		0.3	1.2		0.9					3.3
	$^2D_{3/2}$		0.2		0.4		1.8				
	$^2D_{5/2}$					1.7		2.6			3.3
	$^2F_{5/2}$						0.5		4.4	3.6	
	$^2F_{7/2}$							0.8			4.2
	Q'	0.3	0.7	1.4	0.4	2.6	2.3	3.4	4.4	3.6	10.8

^aCross section was determined by use of experimental branching-ratio data of Hodges (Ref. 14) as the line was too weak for direct determination.

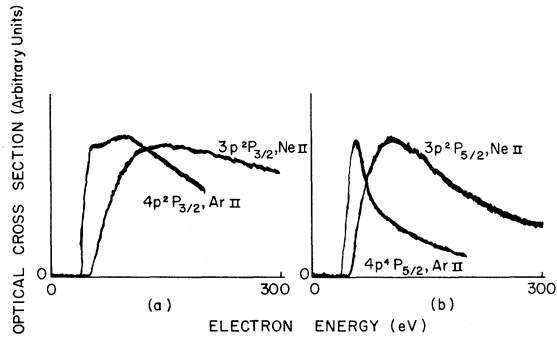


FIG. 7. Comparison of the optical excitation functions of neon and argon for simultaneous excitation and ionization by electron impact.

DISCUSSION

The excitation functions in general were found to be very broad with a slow rise after onset. To illustrate this, Fig. 7 shows a comparison of excitation functions for simultaneous ionization and excitation of argon¹⁵ and neon with similar level designations.

The functions for the doublet levels were broader than those for the quartet levels as expected, since the excitation to the quartet levels involves an exchange between the bombarding electron and one of the atomic electrons, giving rise to a more resonant type of behavior. Also, the quartet functions become more peaked with larger values of J for a given L family.

One approach to explain this behavior of the excitation functions is to assume that heavy mixing occurs between the doublet and quartet levels. This would broaden the quartet functions to some intermediate width, depending on the severity of mixing, between the normally narrow excitation function associated with a pure LS coupled quartet level and the broad excitation function associated with a doublet level.

Sharpton *et al.*¹ have applied this method to the singlet and triplet excitation functions of atomic neon. They expressed the wave function of a state as a linear combination of the LS -basis functions of all states with the J value of that state. The reasoning is that since the total angular momentum is a constant of motion, J is the only good quantum number of any type of coupling scheme which might be used. Hence, the wave function of the state under examination can be written as an expansion of a complete set of eigenfunctions corresponding to the same J value. The LS -basis functions meet this requirement. Using this method, the quantum nature of a state would be a mixture of singlet (or doublet) and triplet (or quartet) components. When this mixing was strong

for a given triplet state, the excitation function of that state was broader than the function of a triplet state with little mixing, since the triplet in the former case takes on a significant portion of the singlet characteristics.

Applying this approach to the Ne II levels, we expect the form of the wave function to be, e.g., for the $3p^4 P_{1/2}$ state as

$$\psi(3p^4 P_{1/2}) = \alpha\psi^{LS}(3p^2 S_{1/2}) + \beta\psi^{LS}(3p^2 P_{1/2}) + \gamma\psi^{LS}(3p^4 P_{1/2}) + \xi\psi^{LS}(3p^4 D_{1/2}), \quad (6)$$

where ψ^{LS} represents the LS -basis wave functions and α , β , γ , and ξ are the mixing coefficients. Large values of α and β contribute to a large mixing and a broadening of the $3p^4 P_{1/2}$ level. For a high- J value such as $\frac{5}{2}$, we expect less broadening since there is only one doublet level with a value J of $\frac{5}{2}$, i.e., $3p^2 D_{5/2}$. This agrees with the excitation function of $3p^4 P_{5/2}$. A similar argument can be stated for the $3p^4 D_{7/2}$ level. In this case, there are no other levels in the (3P) $3p$ family with $J = \frac{7}{2}$ and we expect the $3p^4 D_{7/2}$ excitation function to be quite narrow. From Fig. 2 it may be observed that the $3p^4 D_{7/2}$ excitation function has a more pronounced peak than the other (3P) $3p$ levels. Figure 3 contains the excitation function for the $3d^4 F_{9/2}$ level. No mixing should exist since there are no other $J = \frac{9}{2}$ levels. Accordingly, this level has the most narrow excitation function found in this work. Such an approach does explain the broadness of the quartet functions and the gradual change to a more peaked shape with larger J value.

TABLE V. Level cross sections of the $3p$ levels in units of 10^{-21} cm² at 150 eV.

Level	Cross section	Cascade (%)
$3p^2 S_{1/2}$	6.4	35
$3p^2 P_{1/2}$	77.2	6
$3p^2 P_{3/2}$	163.9	3
$3p^2 D_{3/2}$	18.6	22
$3p^2 D_{5/2}$	19.2	29
$3p^4 P_{1/2}$	5.7	31
$3p^4 P_{3/2}$	8.6	41
$3p^4 P_{5/2}$	10.6	48
$3p^4 D_{1/2}$	3.2	55
$3p^4 D_{3/2}$	3.3	73
$3p^4 D_{5/2}$	9.9	40
$3p^4 D_{7/2}$	7.0	55
$3p'^2 P_{1/2}$	46.9	1
$3p'^2 P_{3/2}$	77.5	7
$3p'^2 D_{3/2}$	14.2	14
$3p'^2 D_{5/2}$	11.0	41
$3p'^2 F_{5/2}$	19.4	30
$3p'^2 F_{7/2}$	30.7	14
$3p''^2 P_{1/2}$	7.4	0
$3p''^2 P_{3/2}$	13.7	0

However, recent spectroscopic work by Persson and Minnhagen³ and Persson⁴ has verified previous experiments^{13,14} that the location of the $3p$ levels are well predicted by LS coupling; this implies that little mixing occurs.

As a possible alternative explanation for the broadness, the shape of these excitation functions may be governed somewhat by the shape of the single-ionization function which has a shape very similar to the $3p^2P_j$ functions. It is reported by von Engel¹⁶ that experiment shows the onset of the ionization function of argon to have a slope of 71 while for neon, only 5.6. From Fig. 7 we see a similar condition holds for the simultaneous ionization and excitation of the two atoms. A review of Latimer and St. John's article¹⁵ shows that all of the argon-ion functions have a much sharper onset than those for the neon ion presented in this paper.

There has been only one theoretical calculation of cross sections for simultaneous ionization and excitation of neon by electron impact. Koozekanani¹⁷ has applied the sudden-perturbation approximation and found the cross section to depend directly upon the ionization function,

$$Q_j = K_j Q_{ion}^+, \quad (7)$$

where j is the state of the ion in question, K_j is

TABLE VI. Comparison of sudden-perturbation calculated cross sections and experimental level cross sections at 150 eV in units of 10^{-21} cm².

Level	Experimental	Sudden perturbation
$3p^2S_{1/2}$	6.4	20.8
$3p^2P_{1/2}$	77.2	138.6
$3p^2P_{3/2}$	163.9	311.1
$3p^2D_{3/2}$	18.6	16.2
$3p^4D_{3/2}$	3.2	0.6

a calculated coefficient dependent on level j but independent of electron energy, and Q_{ion}^+ is the cross section for ionization without excitation. That this relation could be valid only at energies somewhat above onset of Q_j and higher is obvious from the fact that the onset voltage of Q_{ion}^+ is lower than that for Q_j for all j states. The comparison of Q_j with Q_{ion}^+ should be confined to energies which are in excess of several times onset energies. Koozekanani has calculated K for five $3p$ levels. We have used Q_{ion}^+ (150 eV) = 0.70×10^{-16} cm² from the review article by Kieffer and Dunn,¹⁸ and determined the theoretical cross sec-

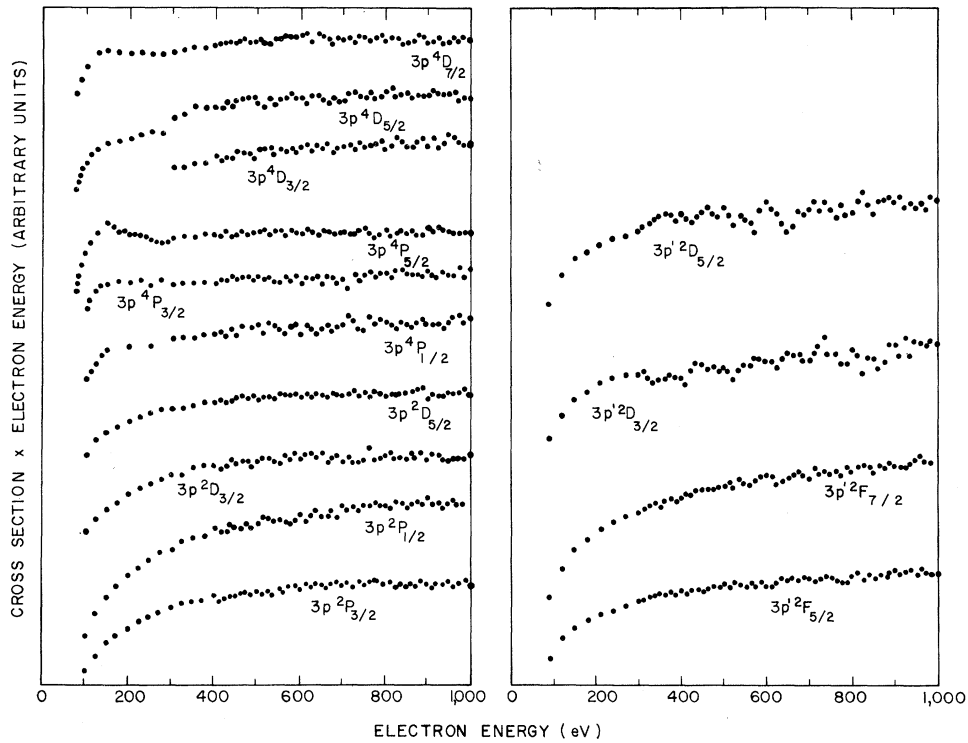


FIG. 8. Optical excitation cross section times electron energy vs electron energy showing the cross sections tend to vary as E^{-1} above 500 eV for the $3p$ levels and the $3p^2D_j$ and $3p^2F_j$ levels.

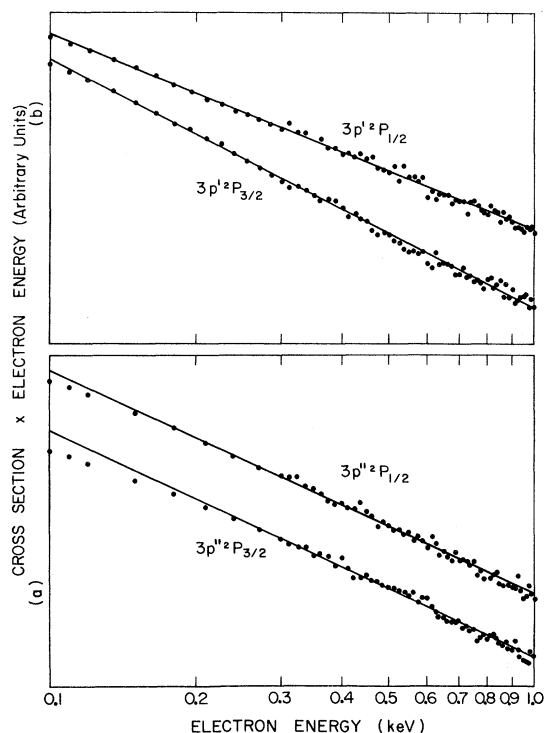


FIG. 9. Electron energy vs optical cross section times electron energy from 0.1 to 1 keV for (a) $3p'^2P_J$ levels and (b) $3p''^2P_J$ levels showing a cross section variation of $(\ln E)/E$.

tions. Table VI compares these results with our experimental values.

HIGH-ENERGY RESULTS AND DISCUSSION

We have examined several of the excitation functions of the $3p$, $3p'$, and $3p''$ levels as well as their cascade components up to 1000 eV. Some of these $3p$ levels are strongly fed by cascade while the $3p'$ levels are affected less, and the $3p''$ levels receive no cascade (see Table V). In preparing the cross-section data for comparison with theory, level excitation functions were obtained by subtracting cascade contributions from the apparent excitation functions. In each case to be presented below, the energy dependence of the apparent and level cross sections were essentially the same. This comes about since an entire family of levels (unprimed, primed, or double primed)

has a set of excitation functions of great similarity. As unprimed (primed, double primed) states cascade into other unprimed (primed, double primed) states, the apparent and level excitation functions of the unprimed (primed, double primed) states have almost the same shape, especially at high energies. This shape additionally is the same as the function of the optical excitation function. We have chosen to analyze the energy dependence of the optical excitation functions rather than of the level excitation functions in order to use raw data. Cascade corrections invariably involve the use of theoretical branching factors and cross sections of weak transitions with their large possible errors.

From Fig. 8(a) it is seen that the optical excitation functions of the $3p$ levels tend to an E^{-1} dependency at around 500 eV and above. This is especially true for the $3p^2P_{3/2}$, $3p^2D_{3/2}$, $3p^2D_{5/2}$, $3p^4P_{5/2}$, $3p^4D_{5/2}$, and $3p^4D_{7/2}$ functions. From Fig. 8(b) we observe no definite trend for the $3p'^2D_J$ and $3p'^2F_J$ levels in the energy range examined, although the curves appear to be leveling out at about 900 or 1000 eV.

Moussa and DeHeer¹⁹ have observed in the simultaneous ionization and excitation of helium an E^{-1} dependence as well. For simultaneous ionization and excitation of argon, Latimer and St. John¹⁵ obtained an E^{-1} dependence for the $4p^2P_J$ levels in the 250 to 700 eV range.

We have, however, observed a $(\ln E)/E$ dependence for functions of the $3p'^2P_J$, and $3p''^2P_J$ levels of the neon ion in the energy range examined. These results are presented in Fig. 9.

If Eq. (7) is valid at elevated energies, the excitation functions should possess an energy dependence identical to the ionization function at higher energies. Bethe²⁰ has predicted a $(\ln E)/E$ dependence for ionization; experiment¹⁸ has verified such a dependence for energies in excess of 300 eV. Hence, the excitation functions for simultaneous ionization and excitation, according to the sudden-perturbation approximation of Koozekanani, should exhibit this $(\ln E)/E$ dependence at high energies. Four levels do follow this dependence. However, since a great majority of the functions examined in this work did not possess a $(\ln E)/E$ dependence, some question still persists on the validity of Eq. (7) and the sudden-perturbation approximation.

*Research supported in part by the Air Force Office of Scientific Research, Office of Aerospace Research, U. S. Air Force under Grants No. AF-AFOSR 252-67 and AF-AFOSR 71-2051.

†Present address: Bethany Nazarene College, Bethany, Okla. 73008.

¹F. A. Sharpton, R. M. St. John, C. C. Lin, and F. E. Fajen, Phys. Rev. A 2, 1305 (1970).

²W. P. Bridges and A. N. Chester, IEEE J. Quantum Electron. QE-1, 66 (1965).

³W. Persson and L. Minnhagen, Arkiv Fysik 37, 273 (1967).

⁴W. Persson, Phys. Scripta 3, 133 (1971).

⁵R. M. St. John, *Methods of Experimental Physics* (Academic, New York, 1969), Vol. 8, p. 27.

⁶J. D. Jobe and R. M. St. John, Phys. Rev. 164, 117

(1967).

⁷P. N. Clout and D. W. O. Heddle, *J. Opt. Soc. Am.* **59**, 715 (1969).⁸J. C. DeVos, *Physica* **20**, 715 (1954).⁹R. H. Garstang, *Monthly Notices Roy. Astron. Soc.* **114**, 118 (1954).¹⁰See, for example, E. U. Condon, and G. H. Shortley, *Theory of Atomic Spectra* (Cambridge U. P., New York, 1953), Eqs. (1) and (3) on pp. 97 and 98.¹¹S. H. Koozekanani and G. L. Trusty, *J. Opt. Soc. Am.* **59**, 1281 (1969).¹²B. F. J. Luyken, *Physica* **51**, 445 (1971).¹³D. W. Koopman, *J. Opt. Soc. Am.* **54**, 1354 (1964).¹⁴D. Hodges, H. Marantz, and C. L. Tang, *J. Opt. Soc. Am.* **60**, 192 (1970).¹⁵I. D. Latimer and R. M. St. John, *Phys. Rev. A* **1**, 1612 (1970).¹⁶A. von Engel, *Ionized Gases* (Clarendon, Oxford, 1965), Table 3.7, p. 63.¹⁷S. H. Koozekanani, *IEEE J. Quantum Electron.* **QE-4**, 59 (1968).¹⁸L. J. Kieffer and J. H. Dunn, *Rev. Mod. Phys.* **38**, 1 (1966).¹⁹H. R. Moustafa Moussa and F. J. DeHeer, *Physica* **36**, 646 (1967).²⁰H. A. Bethe, *Ann. Physik* **5**, 325 (1930).

PHYSICAL REVIEW A

VOLUME 6, NUMBER 1

JULY 1972

Fluctuations in the Energy Loss of 66- and 100-MeV Protons in a Thin Proportional Counter*

G. T. Huetter, R. Madey,[†] and S. M. Yushak*Clarkson College of Technology, Potsdam, New York 13676*

(Received 3 January 1972)

Fluctuations in the energy loss have been measured for 66- and 100-MeV protons passing through a proportional counter filled with 11.0 mg/cm² of a gas mixture of 90% xenon plus 10% methane. The measured values are consistent with the theoretical values determined from the Vavilov theory for energy-loss fluctuations; however, when the Vavilov theory is corrected for the binding effect of the electrons based on the formulation of Shulek *et al.*, the corrected theoretical energy-loss distributions do not agree with the experimental distributions.

I. INTRODUCTION

The theory of fluctuations in the energy loss of heavy charged particles in matter has been developed by Bohr,¹ Landau,² Symon,³ Vavilov,⁴ and others.⁵⁻¹⁰ Landau² has derived an energy-loss distribution function without placing any limits on the magnitude of the energy transferred to an atomic electron. The Vavilov⁴ theory of energy-loss straggling takes into account the kinematic limit to the energy transfer per collision. Both the Landau² and the Vavilov⁴ theories make the approximation that the total energy loss in traversing an absorber is small compared with the initial energy, and that the energy transferred to an atomic electron in a single collision is large compared with the binding energy of the atomic electron. This latter approximation produces a collision spectrum that varies inversely with the square of the kinetic energy transferred to the struck electron. Blunck and Leisegang⁶ and also Shulek *et al.*⁸ have considered distant collisions in which the energy transferred to an atomic electron is comparable with its binding energy. In this energy-transfer region, the collision spectrum is modified by so-called resonance effects. The

Landau² and Vavilov⁴ theories use only the first moment of the resonance cross section. In accounting for the resonant energy transfers during distant collisions, Blunck and Leisegang⁶ extended the theory of Landau,² and Shulek *et al.*⁸ extended the theory of Vavilov⁴ by including the second moment of the resonance cross section.

Igo *et al.*¹¹ measured the statistical fluctuations in ionization by 31.5-MeV protons in a proportional counter filled with 96% argon and 4% carbon dioxide. They found moderate agreement with the Landau theory. Gooding and Eisberg¹² measured the statistical fluctuations in the energy loss of 37-MeV protons over a range of absorber thicknesses from 3.1 to 18.6 mg/cm² of a gas mixture of 96% argon and 4% carbon dioxide. Gooding and Eisberg¹² conclude that the frequency distribution of energy losses of 37-MeV protons agree in shape and full width with the predictions of Symon.³ Murthy and Demeester¹³ used a proportional counter filled with 93% argon and 7% methane to measure the pulse-height distribution of 80-MeV protons. This experiment did not permit distinguishing between the Vavilov⁴ and the Blunck-Leisegang⁶ theories: However, for similar experiments with 1.5- and 4-GeV pions, Murthy and DeMeester¹³